Food Chemistry: X 27 (2025) 102411

Contents lists available at ScienceDirect

Food Chemistry: X

journal homepage: www.sciencedirect.com/journal/food-chemistry-x

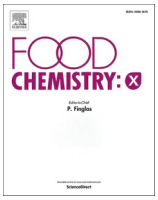

Investigation on appearance, texture, and molecular structure of heat-alkali synergistically induced egg white gel

Song Yang [a,b,c,d], Yan Zhao [a,b,c,d], Na Wu [a,b,c,d], Yao Yao [a,b,c,d], Lilan Xu [a,b,c,d], Shuping Chen [a,b,c,d], Yonggang Tu [a,b,c,d,*]

[a] Jiangxi Key Laboratory of Natural Products and Functional Food, Jiangxi Agricultural University, Nanchang 330045, China
[b] Agricultural Products Processing and Quality Control Engineering Laboratory of Jiangxi, Jiangxi Agricultural University, Nanchang 330045, China
[c] Jiangxi Experimental Teaching Demonstration Center of Agricultural Products Storage and Processing Engineering, Jiangxi Agricultural University, Nanchang 330045, China
[d] Nanchang Key Laboratory of Egg Safety Production and Processing Engineering, Jiangxi Agricultural University, Nanchang 330045, China

ARTICLE INFO

Keywords:
Egg white gel
Heat induction
Alkali induction
Heat-alkali synergistic induction

ABSTRACT

To investigate the effect of heat-alkali synergistical induction on egg white gels, the gels formed from fresh duck egg whites were induced by heating in a water bath at 50 °C, 55 °C, 60 °C and 65 °C for 10 min, followed by the addition of NaOH at concentrations of 4.5 %, 5.0 %, 5.5 %, and 6 % were investigated at the level of appearance, texture, and molecular structure in this study. The appearance, physical and chemical character, textural properties, and molecular structure comprehensive investigation concluded that alkali induction caused heat-induced egg white protein to continue to be denatured, the degree of transparency was increased, part of the free water was converted to bound water, the intermolecular repulsion increased, the microscopic pores increased. The proteins in egg white continued to be crosslinked to form a three-dimensional network structure, creating a stable gel structure.

1. Introduction

The egg white (EW) serves as a widely acknowledged reservoir of exemplary protein, garnering significant attention for its amino acid profile that caters to human nutritional exigencies and easy digestion and absorption (Anton, 2013; Dong & Zhang, 2020). Furthermore, EW boasts noteworthy functional attributes like gelation and foaming (Lv et al., 2022; Sheng et al., 2018). Gelation entails the metamorphosis wherein a substance shifts from a liquid state to a solid form through chemical processes, physical interventions, or other pertinent factors. Within this evolution, fluidic molecules bond, constructing a three-dimensional solid framework that confers gelation upon the material.

Alkalis (Chen et al., 2015; Gao et al., 2020; Zhao et al., 2014), heat (Liu et al., 2020; Yoshinori et al., 1990), and enzymes (Tarhan et al., 2016) constitute a selection of inducers capable of engendering EW gelation. Prevalent techniques include the alkaline-induced creation of transparent EW gel (Gao et al., 2020) and the generation of a milky opaque EW gel through thermal triggers (Li et al., 2018). Diverse incitement avenues prompt gelation via intricate pathways with various supportive forces, thereby engendering distinctions in appearance, consistency, moisture content, and other facets of the resultant gels.

EW gels are divided into two categories based on their morphological characteristics: a clumping gel and a clear gel. Presently, the variance in generating these gel types is commonly attributed to differing rates of protein denaturation and protein aggregation (Zang et al., 2023). When the speed of protein aggregation surpasses the denaturation rate, they give rise to opaque or minimally translucent gels; conversely, transparent gels form otherwise. Elevated-temperature thermal processing yields opaque agglomerates akin to poached eggs, whereas intense alkaline induction yields clear EW gels, reminiscent of preserved eggs.

Preserved egg is a special Chinese food with unique flavor, featuring a distinctive flavor profile that not only tantalizes the taste buds but also aids in digestion (Luo et al., 2020; Zhao et al., 2020). The intricate process of producing preserved eggs involves submerging fresh poultry eggs in a solution comprising alkali, salt, metal compounds, and tea, allowing them to undergo about 40-day pickling period to reach their

* Corresponding author at: Jiangxi Key Laboratory of Natural Products and Functional Food, Jiangxi Agricultural University, Nanchang 330045, China.
E-mail address: tygzy1212@jxau.edu.cn (Y. Tu).

https://doi.org/10.1016/j.fochx.2025.102411
Received 12 November 2024; Received in revised form 7 February 2025; Accepted 23 March 2025
Available online 25 March 2025

state (Cai & Sweeney, 2018; Zhao et al., 2016a). Historically, the traditional method of preparing preserved eggs involved the addition of a specific quantity of PbO into the pickling solution to ensure the integrity of preserved egg white gel. However, due to the health risks associated with PbO, contemporary practices have shifted towards using $CuSO_4$ and $ZnSO_4$ instead of PbO during the processing of preserved eggs. These heavy metal compounds react with sulfur-containing amino acids released during the pickling process, forming sulfides that seal the pores in the eggshell. This sealing mechanism prevents the gelatinous egg white of the preserved egg from undergoing liquefaction. Achievement non-heavy metal pickling technique for preserved eggs stands as a critical hurdle in the industry, given the distinctive role of heavy metal compounds in the pickling solution of preserved eggs, therefore emerging as a central research focus within this domain (Li et al., 2022).

Consequently, this study aimed to implement a heat-alkali synergistic technique aimed at stimulating the creation of duck EW gel and delving into its underlying mechanisms, thereby introducing an innovative strategy for the non-heavy metal processing of preserved eggs. Initially, the duck EW underwent a process of heat induction to transition into a sol state, ensuring that the temperature remained below the complete denaturation threshold of the EW protein to sustain a state of partial fluidity while preventing complete gelation; hence, based on the preliminary test results, temperature parameters ranging from 50 to 65 °C were deemed optimal. Subsequently, the alkali was introduced to induce the gelation process. Upon conducting preliminary experiments, it was noted that insufficient alkalinity failed to achieve complete denaturation of the EW sol post-heat induction, whereas excess alkali concentrations prompted swift liquefaction within a condensed timeframe. Thus, based on the preliminary test results, a NaOH concentration varying between 4.5 % and 6 % was identified as the ideal range, NaOH concentration outside this range can also induce the formation of gels, but the gel state is in a poor form, and is not a rational gel state. The central aim of this exploration was to illuminate the intricate mechanisms behind the collaborative impact of heat and alkali in inducing EW gel formation, while concurrently laying the groundwork for non-heavy metal processing technologies within the realm of preserved eggs.

2. Materials and methods

2.1. Chemicals

Sodium hydroxide (NaOH) was bought from Sinopharm Chemical Reagent Corporation, Ltd. (Shanghai, China). Urea, phosphate buffer reagents were purchased from Solarbio Science & Technology Co., Ltd. (Beijing, China). Glacial acetic acid and methanol were obtained from Xilong Science Co., LTD. (Shantou, China). β-mercaptoethanol (β-ME) and potassium bromide were purchased from Aladdin Biochemical Technology Co., LTD. (Shanghai, China).

2.2. Preparation of heat-alkali synergistically induced EW gels

Fresh duck eggs white were obtained by separating the egg yolk from the fresh duck eggs (65–75 g, from Jiangxi Tianyun Agricultural Development Co.). After magnetic stirring for 30 min, a double gauze was used to filter out any chalazas and eggshells. The resulting EWs were divided into 50 mL beakers, with each beaker containing 20 g of EWs. Subsequently, the EWs were heated in a water bath at temperatures of 50 °C, 55 °C, 60 °C or 65 °C for 10 min before being cooled to room temperature. Subsequent alkali induction, each heat-induced sample received an addition of either a 4.5 %, 5.0 %, 5.5 %, or 6.0 % (*w/v*) NaOH solution; thorough mixing was achieved using a glass rod during this process. The resulting gel formed after adding lye for one hour served as the sample for subsequent analysis.

2.3. Determination of appearance

The EW gel exterior was photographed and observed using a 1200 W pixel camera.

2.4. Determination of pH

The method described by Xue (Xue, Xu, Liao, et al., 2021) was slightly modified to determine gel pH. To ascertain the pH of the supernatant, three grams of EW gel was combined with 27 mL of ultrapure water, homogenized at 15,000 g for 1 min, and then centrifuged at 12,000*g* for 20 min. The pH measurement was conducted utilizing a pH meter from LeiCi Co., headquartered in Shanghai, China.

2.5. Determination of opacity

Park's method (Su-IL & Zhao, 2004) was used with slight modification to determine the opacity of the gel. The EW gel was loaded into a microplate reader and the absorbance value at 600 nm was determined and the opacity was calculated as.

$$\text{Opacity} = \text{Abs}600/\text{t}$$

where t (mm) is the gel height.

2.6. Color measurement

The EW gel was cut into 10 × 10 × 10 mm^3 sized squares and placed in a colorimeter (Hunter Engineering Co., USA) for color analysis to obtain the L*, a*, and b* values of the gel, where L* is the luminance value, a* is the redness-greenness value, and b* is the yellowness-blueness value.

2.7. Measurement of textural properties

Refer to Chen's (Chen et al., 2015) method with slight modifications to determine the textural properties of the gels. EW gels were cut into 10 × 10 × 10 mm^3 sized squares and texture was determined using a texture meter (SMS Co., UK). The parameters were TPA mode, P50 probe, 50 % compression ratio, pre-test, test, and post-test speeds of 2 mm/s, and 5 g trigger force for hardness, springiness, and cohesiveness.

2.8. Determination of swelling ratio

Referring to Ma's (Ma et al., 2018) method, which was slightly modified from it, the swelling ratio of EW gel was determined. The EW gel was immersed in phosphate buffer solution (0.02 M) for 4 h, removed and wiped off the surface water, and then weighed and recorded as m_1. Then freeze-dried for 48 h, weighed, and recorded as m_2. The swelling ratio of gel was calculated using the formula:

$$\text{Swelling ratio} = (m_1 - m_2)/m_2$$

2.9. Determination of moisture distribution

Yu and Liu's method (Liu et al., 2024; Yu et al., 2020) was used with slight modifications to determine the moisture distribution of the gel. Load 2 g of EW gel into a glass bottle and scan T2 using the CPMG pulse sequence of the low-field NMR instrument (NiuMag Co., Shanghai, China). The parameters measured were: pulse width P1 of 17.00 us, waiting time TW of 400.000 ms, RF delay RFD of 0.080 ms, number of samples TD of 15,028, number of accumulations NS of 16, analog gain RG1 of 20.0 db, digital gain DRG1 was 3, the number of echoes NECH was 500, and the echo time TE was 1.000 ms. After sampling, single-component and multi-component analyses were performed with the T2-CPMG fitting program.

2.10. Determination of microstructure

The method of Han (Han et al., 2022) was used with slight modifications to determine the microstructure of the EW gel. The EW gel was cut into 5 × 5 × 5 mm^3 sized squares, frozen and freeze-dried. Then it was put into the scanning electron microscope (FEI Co., USA) for observation. The parameters were: accelerating voltage (EHT) was 20.00 kV, working distance (WD) was 10.0 mm, and magnification was 200.

2.11. Determination of molecular forces

References (Perez-Mzteos et al., 1997) were consulted for the method used in this study with minor modifications. EW gels were sequentially dissolved in four solvents: S1: 0.6 M NaCl solution, S2: 0.6 M NaCl +1.5 M urea solution, S3: 0.6 M NaCl +8 M urea, and S4: 0.6 M NaCl +8 M urea +0.5 M β-ME solution. Approximately 3 g of gel was homogenized with 27 mL of S1 solution at a speed of 12,000 *g* for one minute, followed by centrifugation at the same speed for 20 min to obtain the precipitate from S1. The precipitate obtained from S1 was then homogenized and centrifuged in a similar manner using the same volumes of S2 solution as before; this process was repeated for solvents S3 and S4. The protein content of the resulting supernatant solution was determined using the BCA method. Finally, the supernatant obtained from solvent S4 was dialyzed in solvent S1 to remove any interference from β-ME on protein determination

2.12. Determination of molecular weight distribution

The gel's molecular weight distribution was assessed using SDS-PAGE, following Laemmli and Zhang's (Laemmli, 1970; Zhang et al., 2024) method with minor adjustments. To begin, three grams EW gel was homogenized in a Tris-hydrochloric acid buffer (0.2 M, pH 8.8) at 15,000 g for 1 min and then centrifuged at 12,000 *g* for 15 min. The resulting supernatant solution was collected to determine the protein concentration using Bradford method and adjusted to a concentration of 2mg/mL. A suitable volume of this solution was mixed with an equal volume ratio (1:1, *v/v*) of the 2× loading buffer and heated at 95 °C for 5 min. After another round of centrifugation at 12,000 *g* for 5 min, load 10 μL into the loading wells for electrophoretic analysis alongside an additional injection of protein marker (5 μL) into separate loading wells. The electrophoresis procedure involved applying a constant pressure to the gel, with a voltage level set to achieve up to 200 V. The gel used was primarily composed of a mixture containing 10 % acrylamide. After completion of the electrophoresis process, the gel was taken out and immersed in Coomassie Brilliant Blue R250 staining solution overnight. Subsequently, decolorization was carried out using a solution consisting of glacial acetic acid (5 %) and methanol (25 %).

2.13. Determination of surface hydrophobicity

According to Chelh and Huang's (Chelh et al., 2006; Huang et al., 2022) method, the surface hydrophobicity of the gels was determined using a modified version of their method. In this study, three grams of EW gel was mixed with 17 mL of phosphate buffer solution (0.1 M) and homogenized at a speed of 15,000 *g*. The mixture was then centrifuged at 12,000 *g* for 15 min to obtain the supernatant solution, which was further analyzed for protein concentration using the BCA method and adjusted to a concentration of 5 mg/mL. To assess the surface hydrophobicity, one millilitre of this solution was combined with bromophenol blue solution (1 mg/mL) in a ratio of 200 μg:1 mL and shaken for 10 min at room temperature. After centrifugation at 8000 *g* for another 15 min, the resulting supernatant solution was mixed with phosphate buffer solution (0.1 M) in a ratio of 1:9 (*v*/v). Finally, the absorbance at 595 nm was measured as A_{sample} while using phosphate buffer solution as control $A_{control}$. The amount of bromophenol blue binding can be calculated using the formula: Bromophenol blue binding = 200 × $(A_{control} - A_{sample})/A_{control}$.

2.14. Determination of the secondary structure of proteins

Referring to Shao's (Shao et al., 2017) method and slightly modify the determination of the protein secondary structure of the EW gel. The EW gel was freeze-dried, then dried potassium bromide was added and ground at a ratio of 1:99, and then poured into a mold for pressing. The samples were then placed in a Fourier infrared spectrometer (Thermo Fisher Scientific Co., USA) and scanned at 4000–400 cm^{-1} wavelengths with 64 scans and a resolution of 4 cm^{-1}. The raw spectra were baseline calibrated and smoothed with OMNIC 9.2. Then the second-order derivation of the amide I band (1700–1600 cm^{-1}) was performed and processed by the Savitsky-Golay derivative algorithm to obtain the second-order infrared spectra.

2.15. Statistical analysis of data

The data were expressed using the formation of mean ± variance, plotted using Origin 2022, and analyzed statistically using SPSS 27. Between-group significance tests were performed using Duncan's multiple analysis with a significance level of $p < 0.05$.

3. Results and discussion

3.1. Appearance, pH, opacity and color of egg white gel induced by heat-alkali

Egg-white gels exhibit white and opaque appearance when subjected to high-temperature treatments (Naofumi et al., 1987), while treatment with elevated alkalinity leads to the swift formation of transparent, and faint yellow gels (Chen et al., 2015). The resultant EW gel, achieved through a sequential process of heating followed by alkali introduction, emanated a translucent, light yellow hue (Fig. 1a). Upon closer inspection of the imagery, discernible distinctions in the gels emerged under diverse heat and alkali induction regimes. Specifically, heightened heating temperatures correlated with diminished gel transparency, whereas increased alkali concentrations notably augmented the transparency of the EW gel. Eiser (Eiser et al., 2009) meticulously pickled hard-boiled eggs in a 0.9 M NaOH-0.5 M NaCl solution for 23 days, yielding EWs with a transparent, yellowish complexion akin to the EW gel obtained in this investigation. Huang (Huang et al., 2019) explored the formation of EW gel by immersing duck eggs in a low-alkalinity, high-brine pickling solution, subsequently extracting and individually heating the EWs. As depicted in the visual representations, the EW gel displayed a whitish appearance solely under heat, transitioning into transparent following a 15-day soak in an alkaline solution, radiating a tinge of yellowish-green overall. Similarly, in the investigation by Li (Li et al., 2018), where gel formation was accomplished by mingling duck EWs directly with an alkali/salt mix solutions before subjecting them to high-temperature water heating, the images of the research exhibited EW gels manifesting a reddish-brown, transparent state under intensified alkaline conditions. The EW gel fashioned in the current study shared semblances with that of Huang (Huang et al., 2019), boasting increased transparency in comparison to Li (Li et al., 2018) and a lighter tonality overall presenting a light yellow translucent state. In contemporary research endeavors, some scholars conducted their investigations of egg white gelation by introducing NaCl solutions. In Li's (Li et al., 2018)study, observations of the visual representations illustrating the induction of egg white gelation by alkali/salt and alkali solutions indicated a rise in translucency with the addition of alkali, counteracted by a decrease in translucency upon the inclusion of extra alkali/salt mix solutions. It is thus conjectured that the incorporation of alkali/salt mix solutions may exert an influence, to a certain extent, on the formation of the EW gel.

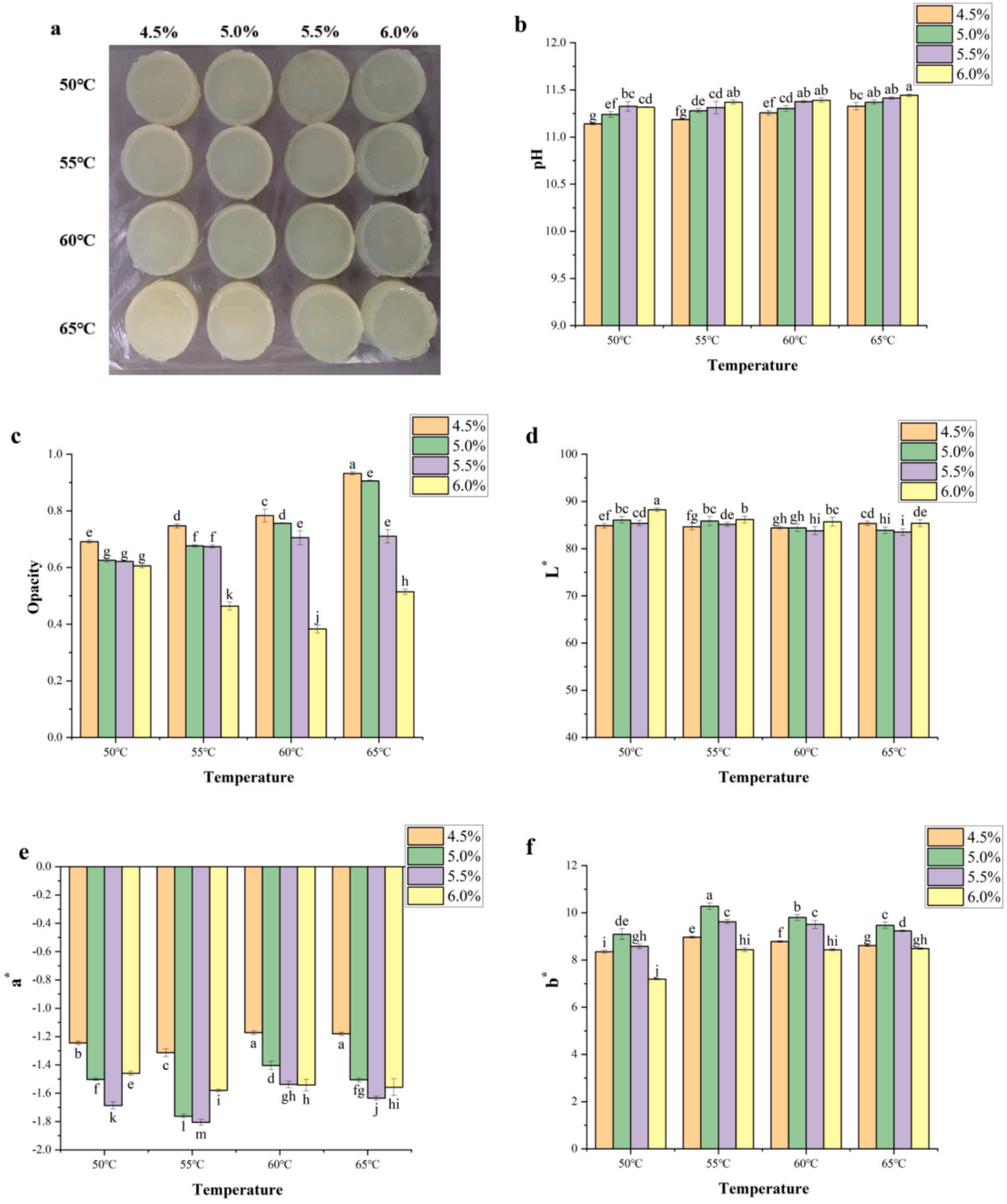

Fig. 1. Changes in appearance (a), pH (b), opacity (c), L* value (d), a* value (e), b* value (f) of EW gels induced by heat-alkali synergy ($p < 0.05$).

The EWs underwent a progressive elevation in heat temperature, coinciding with a general uptrend in gel pH (Fig. 1b). As per insights from Yoshinori (Yoshinori et al., 1990), the application of heat triggered the denaturation of EW proteins, culminating in a globular conformation, heightened hydrophobicity, and increased surface charge. Subsequent alkali introduction facilitated the breakdown of EW proteins through dispersion, alongside the neutralization of positively charged ions on the surface (Xue, Xu, Zhang, et al., 2021). With escalating heating temperatures, there ensued a heightened concentration of denatured proteins and a corresponding increase in ion neutralization, ultimately leading to a pH elevation. The pH levels of the EW gel consistently demonstrated an upward trajectory concomitant with the augmentation of alkali concentration. The addition concentration of alkali increased, but the increase had little effect on the total concentration of EW gel and the overall concentration of the gel. Consequently, the collective pH exhibited a certain rising tendency in tandem with the amplification of alkali concentration.

The opacity of the gel can be ascertained through the absorbance of

the EW gel at 600 nm (Fig. 1c) (Han et al., 2022; Perez-Mzteos et al., 1997). With an escalation in the heating temperature of the EW, there emerged an overarching proclivity towards increased gel opacity ($p < 0.05$). However, in instances where the alkali concentration reached 6 %, the heating of the EW gel displayed an oscillating pattern—initially decreasing ($p < 0.05$) before resuming an ascent ($p < 0.05$) with mounting temperatures—signifying a progressive shift towards transparency under heightened alkalinity. The opacity of the EW gel witnessed a consistent decline ($p < 0.05$) with the augmentation of alkali concentration, underscoring the role of heightened alkalinity in fostering enhanced transparency. Optimal transparency of the EW gel was achieved through a pickling scenario involving a 60 °C induction succeeded by the introduction of 6 % sodium hydroxide, a circumstance aligning harmoniously with the gel's visual manifestation (Fig. 1a). At elevated temperatures, EWs underwent denaturation and aggregation, congealing into opaque, milky-white clusters (Chen et al., 2015). The higher the temperature, the greater the formation of these clusters, thereby augmenting the overall opacity as the EW underwent intense heating. Subsequently, under the influence of alkali, these clusters underwent gradual dispersion. It is posited that the limited dispersal capacity of EW proteins under low alkalinity conditions led to the gradual dissolution of these clusters, whereas elevated alkalinity facilitated a rapid dispersion, resulting in diminished opacity and heightened transparency. In contrast, the lowest opacity and the utmost transparency of the EW gel engendered by the collaborative effects of heat and alkali were observable when 6.0 % alkali was introduced at 60 °C during heating. It is hypothesized that the amount of alkali added under these conditions was therefore just enough to make the agglomerates formed at this temperature more completely dispersed, resulting in a higher degree of gel transparency.

The automated colorimeter is capable of capturing the L*, a*, and b* values of the EW gels (Fig. 1d-f). As the temperature of the EW rose, there was a general decline in the L* value, accompanied by a fluctuating trajectory with an initial rise and subsequent drop in the a* value, and an inverse pattern in the b* value, initially decreasing before ascending ($p < 0.05$). The escalating heating levels gradually diminished the luminosity of the EW gel. The a* value transitioned into negativity, signaling a tint of green, while the b* value shifted to positivity, indicating a hint of yellow. Concomitant with heightened alkalinity was a consistent rise in the L* value. The a* value showcased an initial descent followed by an ascent, reflecting a progression towards green hues succeeded by a regression. Meanwhile, the b* value embarked on a decline initially, culminating in an upward trend subsequently. A comprehensive examination of the gel's visual representation reveals a translucent color palette tending towards yellowish-green as a holistic impression. It is postulated that the color observed during the initial stages of the carbonyl ammonia reaction may be attributed to structural alterations in the glycoprotein arrangement within the EW subsequent to the synergistic interplay of heat and alkali. This could expose certain carbonyl groups, fostering interactions with amino acids and thereby instigating the incipient hues of the Maillard reaction (Huang et al., 2019). Furthermore, it is also possible that fresh duck eggs themselves

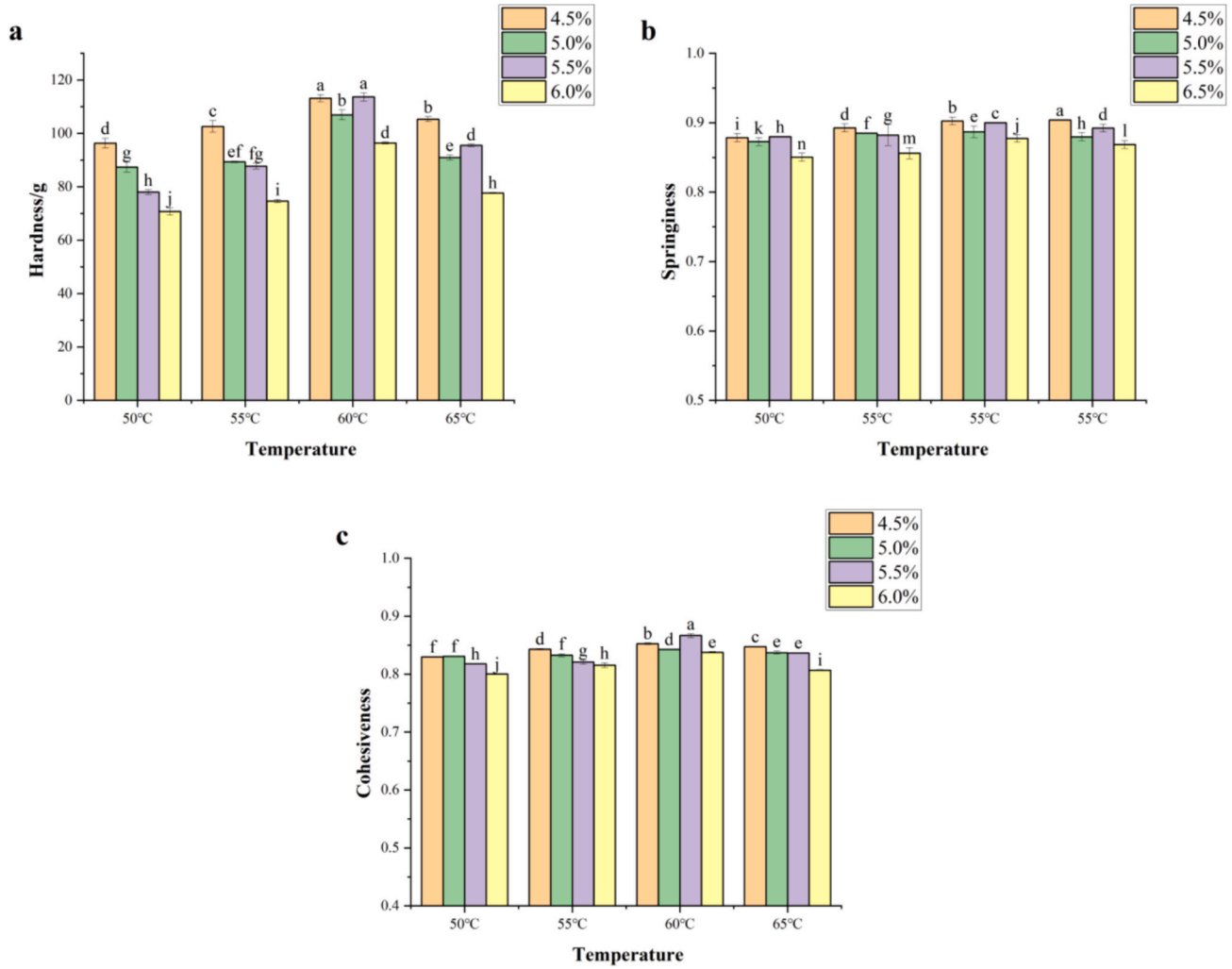

Fig. 2. Changes in the hardness (a), springiness (b), and cohesiveness (c) of EW gel induced by heat-alkali synergy ($p < 0.05$).

contain more riboflavin and carotenoids due to differences in feed feeding, resulting in yellower final EW gels.

3.2. Texture of egg white gel induced by heat-alkali

Texture serves as a pivotal criterion in food, employing simulations of mastication akin to human oral processing, encompassing compression, tension, and other mechanical assessments to unveil properties like hardness, springiness, and cohesiveness of food. The gel's hardness (Fig. 2a), springiness (Fig. 2b), and cohesiveness (Fig. 2c) exhibited an initial increase followed by a subsequent decrease with rising temperatures. The hardness of the gel can be linked to the influence of electrostatic interactions. Through heat-induced depolymerization and consequent aggregation, EW proteins underwent denaturation, unveiling hydrophobic domains. In an alkaline milieu, protein entities bore a significant array of negative charges, intensifying electrostatic repulsion among these molecules and thereby heightening gel hardness (Cai and Sweeney, 2018). The increased heating temperature of the EW under the same alkalinity led to a higher exposure of hydrophobic groups; at the same time, the greater the electrostatic repulsion force, the greater the hardness ($p < 0.05$). Furthermore, these hydrophobic groups facilitated some degree of cross-linking between gels.

Enhanced springiness and cohesiveness within the gel stemmed from a cohesive and intricate gel framework continuously maturing. EWs, subjected to elevated temperatures, unveil concealed sulfhydryl groups within proteins, particularly noteworthy in alkaline settings, actively engaging in disulfide bond formation, thereby fortifying protein tertiary structures. At the pinnacle of heat intensity, excessive electrostatic repulsion triggers protein refolding, submerging certain hydrophobic grouping, correlating with a subsequent dip ($p < 0.05$) in hardness, springiness, and cohesiveness.

With increasing alkalinity, the gel's hardness gradually diminished ($p < 0.05$), while springiness and cohesiveness manifested an initial decline ($p < 0.05$) followed by an elevation ($p < 0.05$). This phenomenon was conceivably linked to pH escalation (Fig. 1b), which neutralized the protein surface charge and thereby contributing to a decline in hardness. Notably, the superior hardness, springiness, cohesiveness, and peak transparency of the EW gels materialized when heated to 60 °C and 65 °C with a 5.5 % alkali concentration. At this juncture, a synergistic interplay of heat and alkali was presumed, facilitating optimal gel network cross-linking and thereby showcasing heightened gel strength.

3.3. Swelling ratio of egg white gel induced by heat-alkali

Swelling epitomizes a foundational characteristic of gels, wherein immersion in a buffering medium elicits water uptake, prompting cross-linking and structural contractions within the gel's lattice. Attainment of a swelling equilibrium signifies the delicate interplay between absorption and contractile forces (He et al., 2023). Gels with heightened cross-linkages inherently harbor superior water content, impeding water absorption. Conversely, gels characterized by lesser cross-linking exhibit augmented porosity, facilitating enhanced water retention. Hence, a negative correlation emerges: augmented gel cross-linking correlates with diminished swelling ratios, whereas a decrease in cross-linking engenders heightened swelling ratios.

The swelling ratio of EW gels witnessed an initial decline followed by a subsequent rise as temperatures escalated (Fig. 3). Similarly, the overall gel swelling exhibited an initial elevation succeeded by a decline with augmented alkalinity concentrations. Noteworthy, the most minimal EW gel swelling was identified upon heating at 60 °C in the presence of a 5.5 % alkalinity concentration ($p < 0.05$). This suggested a fluctuating trend where the degree of cross-linking in EW gels experienced an initial surge followed by a decrease with mounting temperatures while showing an inverse pattern with escalating alkalinity introduction.

When subjected to a regimen involving heating at 60 °C paired with a 5.5 % alkali concentration, a marked reduction in the swelling ratio was discerned, indicative of an optimal level of gel cross-linking attained under these specific conditions. This phenomenon hinted at potential synergistic effects between heat and alkali, accentuating the structural fortitude of the gel network compared to alternative scenarios.

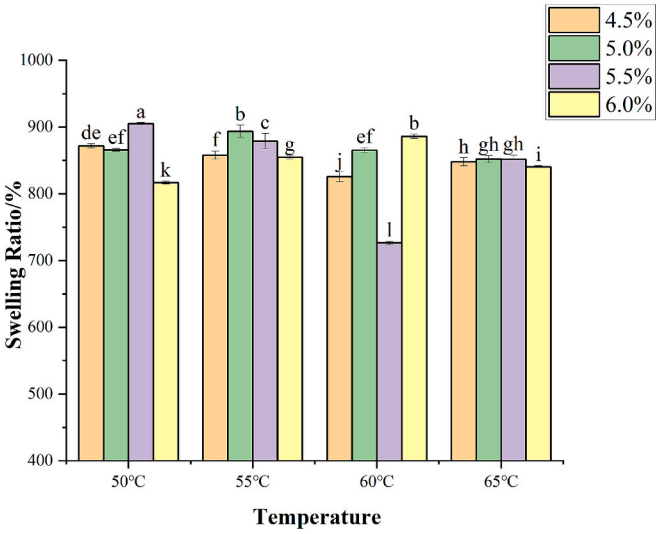

Fig. 3. Swelling ratio of EW gel induced by heat-alkali synergy ($p < 0.05$).

3.4. Moisture distribution of egg white gel induced by heat-alkali

Low-field NMR mainly detects H protons, and the samples containing H are stimulated by a specific frequency to generate NMR signals, corresponding to the two main parameters T1 and T2. The relative contents of free and bound water can be obtained by T2 relaxation spectra. In the spectrum, with the increase in peak time, it can be considered that the water bond is less tight (Xue, Xu, Liao, et al., 2021). Conventionally, a T2 peak below 20 ms denotes water in a bound state, while a range of 20 ms to 200 ms signifies water that is not easily mobile, with T2 values surpassing 200 ms indicative of free water.

With the increase of heating temperature, the overall trend of immobile water in the gel first decreased and then increased (Fig. 4). The denaturation and coalescence of proteins in EW yielded a dense structure impeding water flow. This gel harbors bound water, contributing to a gel matrix preserving pores upon alkaline infusion. Nonetheless, the water retention capability of gels was constrained under high-temperature regimes. As pore dimensions of the gel matrix expanded, not all bound water remained trapped within, transforming into immobile water. With increased alkalinity, a fluctuation of moisture was observed in the gel, juxtaposed with a decline followed by an ascent, suggesting that the decrease in immobile water might signify a transition to bound water.

Upon subjecting EW to specific temperatures, moisture was ensconced within gel blocks. Augmenting alkali concentrations intensified crosslinking within the gel network, boosting water retention potential. Nevertheless, excessive pore enlargement could hamper crosslinking and diminished water-retention prowess. The holistic water content distribution aligned with the color variance (Fig. 1e), potentially tethered to the fluctuating behavior of immobile water due to light scattering attributes (Zhou et al., 2023).

3.5. Microstructure of egg white gel induced by heat-alkali

The microstructure of EW gel can be unveiled through scanning electron microscopy. Findings unveiled a gradual enlargement in gel pore dimensions in tandem with heightened EW heating temperatures (Fig. 5). Furthermore, the pore configuration evolved from an initial heterogeneous state towards denser homogeneity before eventually

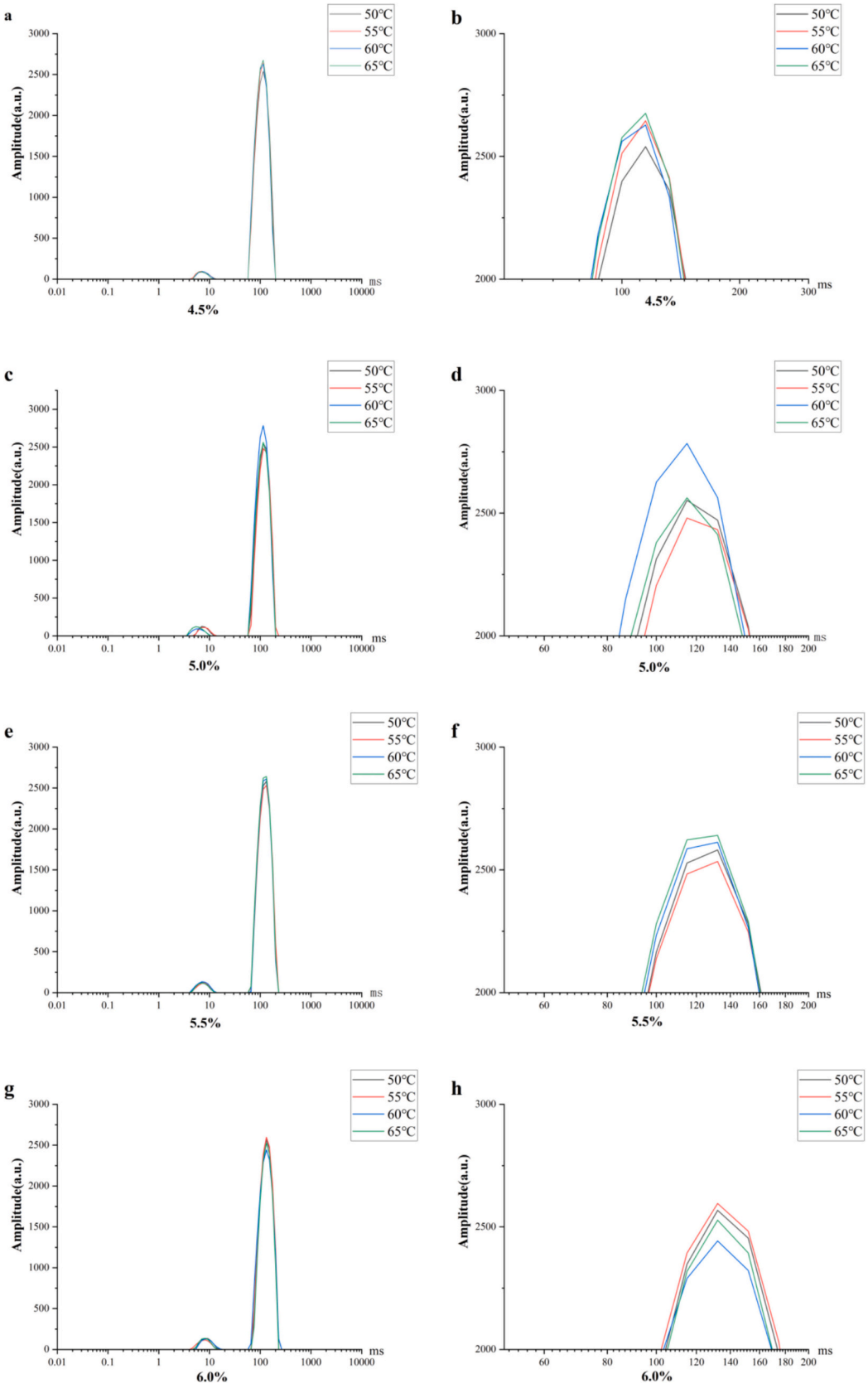

Fig. 4. Changes of water distribution in EW gel induced by heat-alkali synergy.

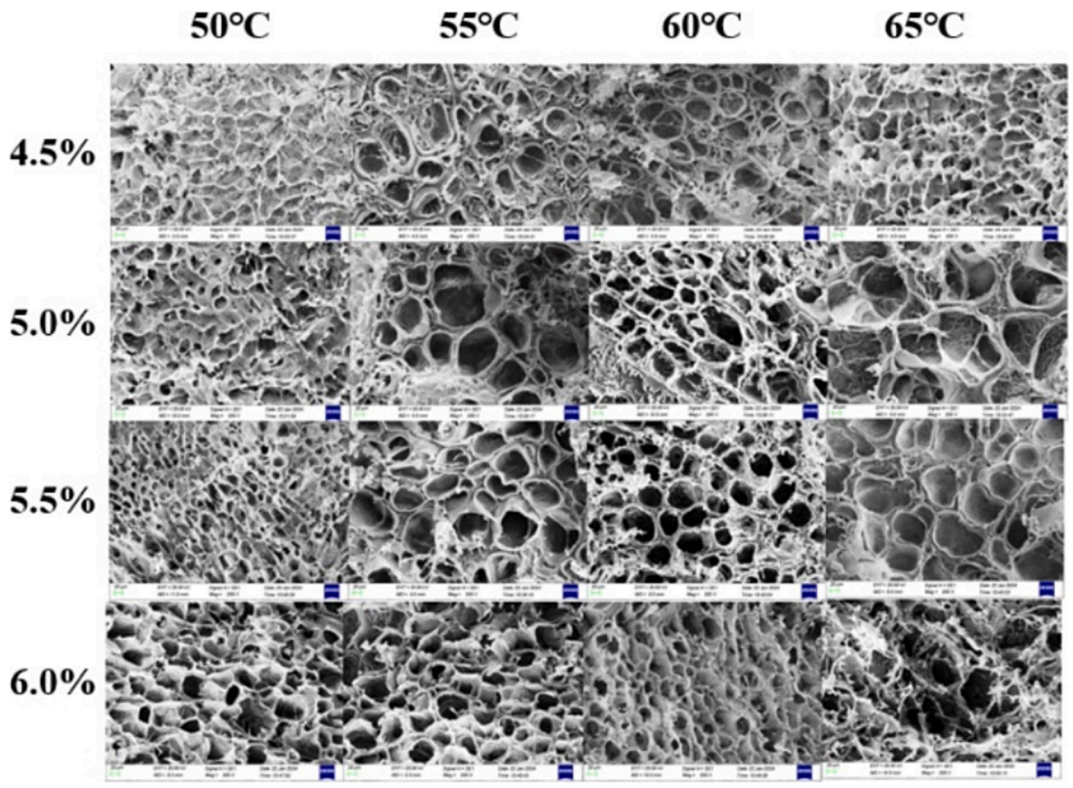

Fig. 5. Electron micrograph of EW gel formed by heat-alkali synergy (200×).

transitioning to a more relaxed state. Yao's research (Yao et al., 2022) delving into EW heating treatments revealed a direct correlation between elevated heating temperatures and the increasingly orderly micro-arrangement of the ensuing gel. The heat-driven denaturation and congregating of EW proteins, under the facilitation of alkali, induced a pH surge. This escalation led to a gradual reinforcement of repulsive forces amidst proteins, triggering a widening of inter-protein spaces. Subsequently, progressive compaction of protein layout ensued until excessive repulsion upset the initial compact configuration, ushering in a looser alignment—encompassing the hardness of gel (Fig. 2a) as well. This metamorphosis might also be linked to the isoelectric point of proteins, marking where protein aggregation and precipitation materialize. As the pH deviated from this pivotal point, the haphazard protein aggregation diminished, linear alignment amplified, and pore dimensions expanded (Huang et al., 2019).

The microstructural portrayal resonated with the moisture distribution findings (Fig. 4), intimating a scenario where denser pores correlate with heightened cross-linking, enhancing water entrapment—an observation also harmonizing with gel swelling ratio (Fig. 3).

3.6. The molecular force of egg white gel induced by heat-alkali

The gel manifests distinct types of protein bonding delineated as follows: S1 embodies ionic bonding, S2 epitomizes hydrogen bonding, S3 embodies hydrophobic interactions, and S4 signifies disulfide bonding (Fig. 6). Initial heating temperatures spurred an increment in the collective proportion of S1 within the gel, succeeded by a subsequent descent. Correspondingly, there was an initial rise followed by a decline in the overall S2 ratio. Conversely, the aggregate proportion of S3 exhibited an initial decline before progressively ascending. Simultaneously, the S4 proportion exhibited a gradual augmentation.

With regard to alkali concentration, elevating its levels triggered an overall escalation in the percentage of S1, accompanied by a rise in the proportion of S2. Nonetheless, for S3, an initial surge followed by a decline was observed with increasing alkali concentrations, whereas a decrease was noted for S4. Chen's findings (Chen et al., 2015) underscored the pivotal roles played by both ionic and disulfide bonds in the genesis of EW gels induced by alkali inductions among the assorted forces examined, hydrogen bonding and hydrophobic interactions made

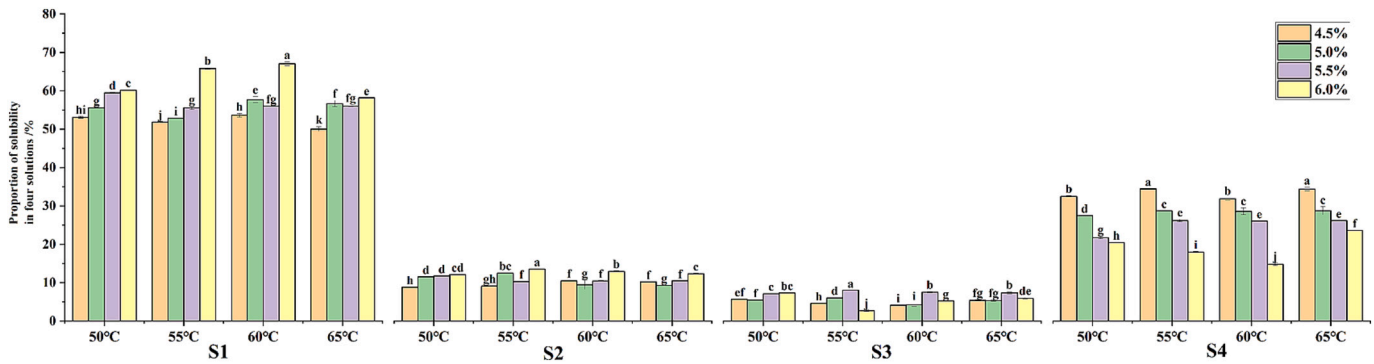

Fig. 6. Percentage of the protein content of EW gels induced by heat-alkali synergy in four solubilizers ($p < 0.05$).

comparatively minor contributions to this progression.

Moreover, when EW gels congealed within the temperature range of 55–65 °C under a base concentration of 5.5 %, they exhibited distinctive attributes diverging from other cohorts: diminished proportions of ionic and hydrogen bonding but amplified percentages of hydrophobic interactions were evident under these circumstances. This likely elucidates why these gels showcased heightened transparency (Fig. 1c), augmented hardness, and cohesiveness (Fig. 2), and more tightly knit protein structures (Fig. 5).

3.7. SDS-PAGE of egg white gel induced by heat-alkali

The fundamentals of electrophoresis hinge upon the denaturation and disassembly of proteins and SDS under elevated temperatures during pre-treatment. Throughout electrophoresis, proteins aggregate initially within the stacking gel, followed by the migration of proteins bearing diverse charges within the separating gel. The velocity of migration is contingent upon the molecular weight of the protein, facilitating the segregation and verification of its protein constitution. Within Fig. 7, the Molecular Weight Marker bands span a spectrum from 195 to 8 kDa, arrayed in descending sequence.

Depending on the molecular weights of distinct proteins, those segregated in the EW gel were broadly classified from base to apex as low molecular weight proteins—comprising lysozyme (14.3–17 kDa), ovalbumin (28 kDa), egg albumin (45 kDa), ovotransferrin (70–78 kDa), and higher molecular weight proteins. Discernibly, the bands transpire from deep to pale hues, with the darkest and thickest ovalbumin bands can be seen more clearly in the figure because EW has the highest ovalbumin content, undergoing heat denaturation into S-ovalbumin at 82 °C. The thicker, darker-hued bands occupying greater molecular weights likely mirror the initial denaturation and disassembly of EWs under thermal conditions due to electrostatic and hydrophobic interactions (Tarhan et al., 2016). Subsequently, EWs reassemble through aggregation, culminating in the formation of protein conglomerates at higher molecular weights under heightened temperatures, hence the discernible darker bands. The faintest and nearly imperceptible bands pertain to lysozyme due to its lower abundance in EWs and thermal instability within alkaline settings. Collectively, as alkalinity escalated, the bands substantially thinned out and lightened in coloration. Notably, the elevated alkalinity charts revealed faint bands at a lower molecular weight of 8 kDa, intimating that heightened alkalinity disintegrated EW proteins into petite molecular protein peptides.

3.8. Surface hydrophobicity of egg white gel induced by heat-alkali

The constitution of proteins is widely acknowledged to encompass an array of amino acids, spanning both hydrophilic and hydrophobic variants. Ordinarily, within EW proteins, hydrophobic amino acids are ensconced centrally, forming a hydrophobic domain. When the denaturation of proteins transpires, the spatial arrangement of the protein undergoes alteration, leading to the exposure of the hydrophobic region. Consequently, the extent of transformation in protein conformation can be delineated by assessing the protein's hydrophobicity (Totosaus et al., 2002). The hydrophobicity of a protein can be gauged by the quantity of bromophenol blue it captures, as this substance, possessing a color-emanating attribute, selectively adheres to amino acid residues within hydrophobic clusters. The heightened retention of bromophenol blue correlates to an elevated degree of hydrophobicity exhibited by the protein.

The gel evinced an overarching upward trajectory as the temperature of the EW surged during heating (Fig. 8). Moreover, as alkalinity intensified, the gel initially demonstrated an upward trend succeeded by a subsequent decline. Additionally, as both temperature and alkalinity

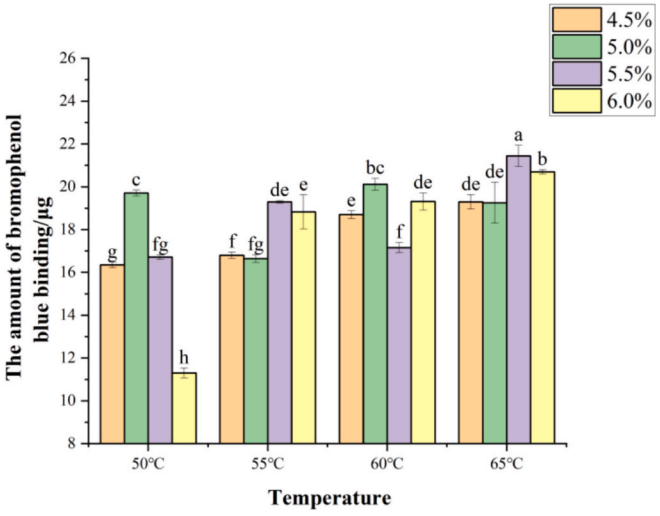

Fig. 8. Bromophenol blue binding content in EW gel induced by heat-alkali synergy ($p < 0.05$). (For interpretation of the references to color in this figure legend, the reader is referred to the web version of this article.)

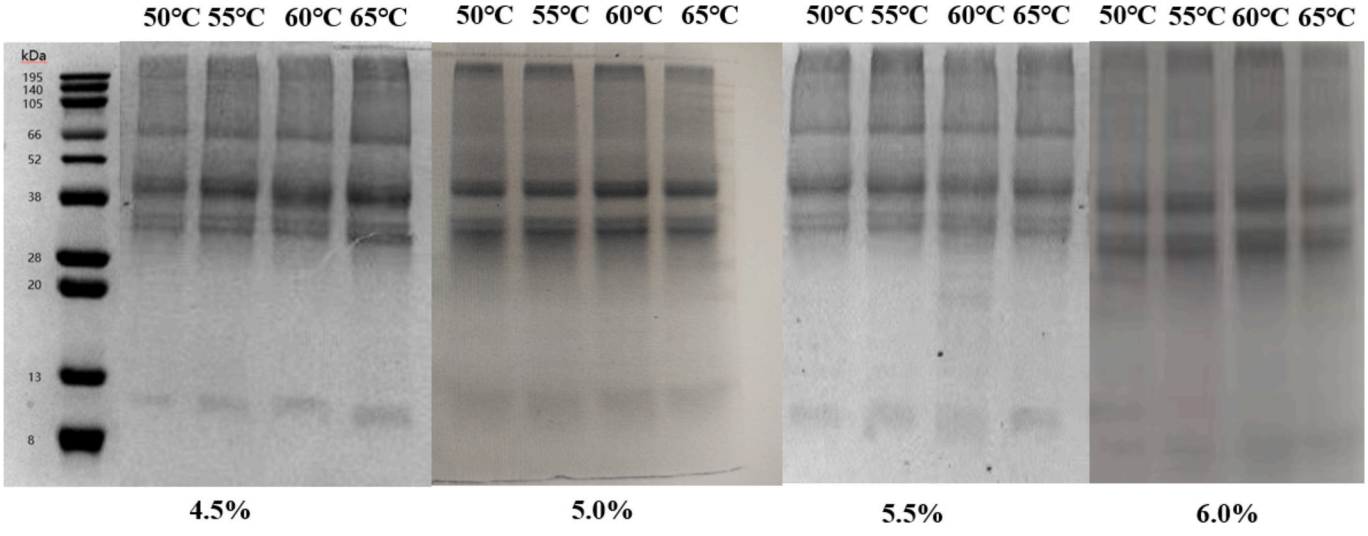

Fig. 7. SDS-PAGE electrophoresis of EW gel induced by heat-alkali synergy.

escalated, transformations ensued in the spatial configuration of proteins. Subsequently, erstwhile concealed hydrophobic clusters within protein molecules gradually surfaced, effectively amplifying the gel's surface hydrophobicity.

Prolonged exposure to alkali instigated ongoing alterations in the molecular architecture of proteins, encompassing modifications in their secondary and tertiary structures. This process engendered protein folding and interlinking, fostering the inclusion and sequestration of hydrophobic clusters, thereby diminishing the surface hydrophobicity of the gel. Subsequent to exposure to a 5.5 % alkali concentration at 60 °C, the gel's hydrophobicity underwent a noteworthy decline, indicative of enhanced sequestration of hydrophobic clusters within the proteins in gel, alongside improved interconnection and folding of molecules. This observation harmonized with both the gel texture index (Fig. 2) and swelling ratio (Fig. 3).

3.9. Infrared spectrum of egg white gel induced by heat-alkali

The interaction of molecules with specific infrared wavelengths instigates transitions in their vibrational and rotational energy states, thereby facilitating the generation of an infrared absorption spectrum for substances upon detection. Within the realm of proteins, the scrutiny of the amide I band (1700–1600 cm^{-1}) in the infrared spectrum holds paramount significance as it encapsulates distinct alterations in the secondary structure of proteins, encompassing β-sheet (1640–1610 cm^{-1}), random coils (1650–1640 cm^{-1}), α-helix (1660–1650 cm^{-1}), and β-turn (1670–1660 cm^{-1}). It was conventionally posited that the α-helix and β-sheet regions of proteins harbor a more abundant presence of hydrogen bonds, pivotal in fortifying the structural integrity of proteins (Gu et al., 2008; Levy-Moonshine et al., 2009), while β-turns and random coils underscore the flexibility of proteins.

Observing Fig. 9, it is discernible that the elevation of heating temperature in EW incrementally amplified and subsequently diminished β-sheet, concomitant with a prevailing augmentation in random coils, and a waxing and waning pattern in α-helices, aligning with an overarching surge in β-turns. Coupled with the intermolecular forces (Fig. 6), hydrogen bonding within the gel initially intensified and subsequently diminished with escalating temperatures, thus precipitating an initial fortification followed by a decline in gel stability.

As the alkalinity escalated, β-sheet underwent a cyclic increase and decrease, random coils exhibited an inversely proportional trend, α-helices demonstrated an overarching decline, and the angle of β-turn oscillated between augmentation and reduction. Correspondingly, the aggregate content of the secondary structure evinced a tendency of initial ascent followed by a descent. Synthesizing with microstructural intricacies (Fig. 5) and the surface hydrophobicity of proteins (Fig. 8), it is postulated that the introduction of alkali catalyzed the folding and interlinking of proteins, thereby fostering a well-ordered arrangement of

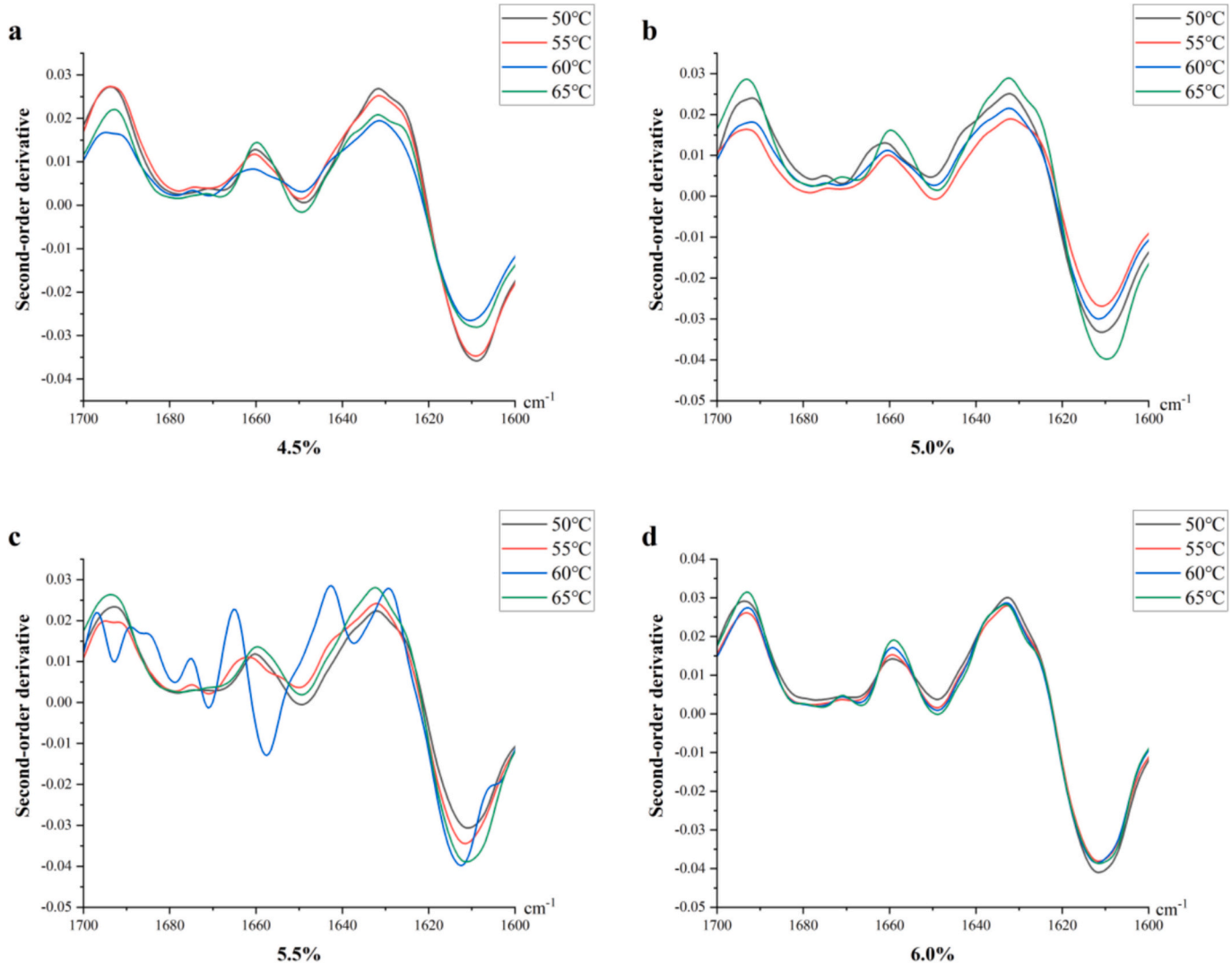

Fig. 9. Fourier infrared second-order derivative spectra of EW gels induced by heat-alkali synergy.

regular secondary structures, consequently augmenting the secondary structure content.

Conversely, excessive alkali infusion under conditions of heightened alkalinity engendered an elevation in gel pH, an uptick in electrostatic repulsion, a declination in linear alignment, and aggregation. Notably, under the influence of a 5.5 % alkali concentration at 60 °C, a discernable red shift surfaced at 1650 cm^{-1} and 1690 cm^{-1}, indicating a directional shift towards lower frequency absorption peaks (Zhao et al., 2016b). Plausibly, under these circumstances, the secondary structure of the EW gel underwent a metamorphosis, possibly witnessing the conversion of certain β-turns into stable α-helices, and sectional random coils transitioning into stable β-sheet. This could elucidate the heightened degree of interlinking (Fig. 3) and the uniform, compact microscopic porosity (Fig. 5) witnessed under such conditions.

4. Conclusion

The investigation delved into the appearance attributes, textural characteristics, and molecular structure of the gel produced from the confluence of heating and alkali induction on egg white. This study sheds light on the mechanism underpinning the formation of the egg white gel. Both heat-induced and alkaline-induced gels exert substantial influence; however, their impacts diverge. Elevation in heating temperature triggers protein denaturation and depolymerization, laying bare hydrophobic entities and augmenting the presence of ionic forces at the surface. Consequently, the electrostatic repulsion intensifies, resulting in heightened firmness and an augmented interstice within the gel framework. Conversely, heightened alkalinity prompts proteins to undergo stochastic aggregation, transitioning into a structured alignment due to the deviation of pH from its isoelectric point. This culminates in an improved elasticity and coherence of proteins, with secondary structures marked by folding interconnections gravitating towards stabilization.

It is hypothesized that the formation of egg white gels is synergistically induced by heat and alkali. Heat induction first denatures and unfolds the globular proteins, which fold again at higher temperatures, but the hydrophobic core continues to be exposed; subsequent alkali induction causes them to continue to undergo denaturation, and the protein structure rearranges itself to form an ordered porous network structure, with the water evenly distributed between the proteins and appearing transparent.

Nevertheless, elevated temperatures and increased alkalinity exert adverse effects on the overall gel performance. The optimal conditions for the formation of an egg white gel entail heating at 60 °C for 10 min coupled with a NaOH concentration of 5.5 %. Under these circumstances, a concurrence of heat-alkali effects unfolds, where electrostatic repulsion attains an optimal equilibrium, yielding heightened translucency and robustness characterized by a homogeneous and dense network of pores within the gel, alongside a pronounced degree of interlinking ensuring commendable stability.

The introduction of the green, safe, and environmentally sustainable heat-alkali synergistic induction methodology holds promise for its integration in the practical production of preserved eggs devoid of heavy metal compounds, paving the way for further exploration through research endeavors.

CRediT authorship contribution statement

Song Yang: Writing – original draft, Methodology, Investigation, Formal analysis, Data curation, Conceptualization. **Yan Zhao:** Writing – review & editing, Supervision, Resources, Project administration, Formal analysis, Data curation, Conceptualization. **Na Wu:** Project administration, Formal analysis, Conceptualization. **Yao Yao:** Supervision, Formal analysis. **Lilan Xu:** Supervision, Formal analysis, Conceptualization. **Shuping Chen:** Supervision, Formal analysis, Conceptualization. **Yonggang Tu:** Writing – review & editing, Supervision, Resources, Project administration, Methodology, Formal analysis, Data curation, Conceptualization.

Declaration of competing interest

The authors declare that they have no known competing financial interests or personal relationships that could have appeared to influence the work reported in this paper.

Acknowledgments

We gratefully acknowledge the support provided by the National Natural Science Foundation of China (Grant Nos. 32260608 and 32472395), the Jiangxi Provincial Outstanding Youth Fund (Original Exploration Category) Project(20224ACB215008), the Training Project of High-level and High-skilled Leading Talents of Jiangxi Province (29202300002) and the Jiangxi Provincial Key Research and Development Project (20232BBF60025).

Data availability

The data that has been used is confidential.

References

Anton, M. (2013). Egg yolk: Structures, functionalities and processes. *Journal of the Science of Food and Agriculture, 93*(12), 2871–2880. https://doi.org/10.1002/jsfa.6247

Cai, J., & Sweeney, A. M. (2018). The proof is in the Pidan: Generalizing proteins as patchy particles. *ACS Central Science, 4*(7), 840–853. https://doi.org/10.1021/acscentsci.8b00187

Chelh, I., Gatellier, P., & Santé-Lhoutellier, V. (2006). Technical note: A simplified procedure for myofibril hydrophobicity determination. *Meat Science, 74*(4), 681–683. https://doi.org/10.1016/j.meatsci.2006.05.019

Chen, Z., Li, J., Tu, Y., Zhao, Y., Luo, X., Wang, J., & Wang, M. (2015). Changes in gel characteristics of egg white under strong alkali treatment. *Food Hydrocolloids, 45*, 1–8. https://doi.org/10.1016/j.foodhyd.2014.10.026

Dong, X., & Zhang, Y. Q. (2020). An insight on egg white: From most common functional food to biomaterial application. *Journal of Biomedical Materials Research Part B: Applied Biomaterials, 109*(7), 1045–1058. https://doi.org/10.1002/jbm.b.34768

Eiser, E., Miles, C. S., Geerts, N., Verschuren, P., & MacPhee, C. E. (2009). Molecular cooking: Physical transformations in Chinese 'century' eggs. *Soft Matter, 5*(14). https://doi.org/10.1039/b902575h

Gao, X., Yao, Y., Wu, N., Xu, M., Zhao, Y., & Tu, Y. (2020). The sol-gel-sol transformation behavior of egg white proteins induced by alkali. *International Journal of Biological Macromolecules, 155*, 588–597. https://doi.org/10.1016/j.ijbiomac.2020.03.209

Gu, B., Zhang, F. S., Wang, Z. P., & Zhou, H. Y. (2008). The solvation of NaCl in model water with different hydrogen bond strength. *Journal of Chemical Physics, 129*, Article 184505. https://doi.org/10.1063/1.3002485

Han, T., Xue, H., Hu, X., Li, R., Liu, H., Tu, Y., & Zhao, Y. (2022). Combined effects of NaOH, NaCl, and heat on the gel characteristics of duck egg white. *Lwt, 159*. https://doi.org/10.1016/j.lwt.2022.113178

He, J., Sun, Y., Gao, Q., He, C., Yao, K., Wang, T., … He, Y. (2023). Gelatin Methacryloyl hydrogel, from standardization, performance, to biomedical application. *Advanced Healthcare Materials, 12*(23). https://doi.org/10.1002/adhm.202300395

Huang, Q., Liu, L., Wu, Y., Huang, X., Wang, G., Song, H., … Luo, P. (2022). Mechanism of differences in characteristics of thick/thin egg whites during storage: Physicochemical, functional and molecular structure characteristics analysis. *Food Chemistry, 369*, Article 130828. https://doi.org/10.1016/j.foodchem.2021.130828

Huang, X., Li, J., Chang, C., Gu, L., Su, Y., & Yang, Y. (2019). Effects of NaOH/NaCl pickling on heat-induced gelation behaviour of egg white. *Food Chemistry, 297*. https://doi.org/10.1016/j.foodchem.2019.06.006

Laemmli, U. K. (1970). Cleavage of structural proteins during the assembly of the head of bacteriophage T4. *Nature, 227*, 680–685. https://doi.org/10.1038/227680a0

Levy-Moonshine, A., Amir, E.-A. D., & Keasar, C. (2009). Enhancement of beta-sheet assembly by cooperative hydrogen bonds potential. *Bioinformatics, 25*(20), 2639–2645. https://doi.org/10.1093/bioinformatics/btp449

Li, A., Wang, Y., Zhang, D., Liu, S., & Ye, Y. (2022). Formation of high-elasticity and high-strength semitransparent ovalbumin gel induced by alkali-heat treatment. *International Journal of Food Properties, 25*(1), 907–923. https://doi.org/10.1080/10942912.2022.2070201

Li, J., Zhang, Y., Fan, Q., Teng, C., Xie, W., Shi, Y., … Yang, Y. (2018). Combination effects of NaOH and NaCl on the rheology and gel characteristics of hen egg white proteins. *Food Chemistry, 250*, 1–6. https://doi.org/10.1016/j.foodchem.2018.01.031

Liu, J., Li, X., Jing, R., Huang, X., Geng, F., Luo, Z., … Huang, Q. (2024). Effect of prolonged cooking at low temperatures on the eating quality of Tibetan pork: Meat

quality, water distribution, and microstructure. *Food Quality and Safety, 8*. https://doi.org/10.1093/fqsafe/fyae025

Liu, X., Wang, J., Huang, Q., Cheng, L., Gan, R., Liu, L., … Geng, F. (2020). Underlying mechanism for the differences in heat-induced gel properties between thick egg whites and thin egg whites: Gel properties, structure and quantitative proteome analysis. *Food Hydrocolloids, 106*. https://doi.org/10.1016/j.foodhyd.2020.105873

Luo, W., Xue, H., Xiong, C., Li, J., Tu, Y., & Zhao, Y. (2020). Effects of temperature on quality of preserved eggs during storage. *Poultry Science, 99*(6), 3144–3157. https://doi.org/10.1016/j.psj.2020.01.020

Lv, X., Huang, X., Ma, B., Chen, Y., Batool, Z., Fu, X., & Jin, Y. (2022). Modification methods and applications of egg protein gel properties: A review. *Comprehensive Reviews in Food Science and Food Safety, 21*(3), 2233–2252. https://doi.org/10.1111/1541-4337.12907

Ma, X., Xu, T., Chen, W., Qin, H., Chi, B., & Ye, Z. (2018). Injectable hydrogels based on the hyaluronic acid and poly (γ-glutamic acid) for controlled protein delivery. *Carbohydrate Polymers, 179*, 100–109. https://doi.org/10.1016/j.carbpol.2017.09.071

Naofumi, K., Hajime, H., & Etsushiro, D. (1987). Heat-induced and transparent gel prepared from hen egg ovalbumin in the presence of salt by a two-step heating method. *Agricultural and Biological Chemistry, 51*, 771–778. https://doi.org/10.1080/00021369.1987.10868108

Perez-Mzteos, M., Lourenco, H., Montero, P., & Borderias, A. J. (1997). Rheological and biochemical characteristics of high-pressure- and heat-induced gels from blue whiting (*Micromesistius poutassou*) muscle proteins. *Journal of Agricultural and Food Chemistry, 45*, 44–49. https://doi.org/10.1021/jf960185m

Shao, Y., Zhao, Y., Xu, M., Chen, Z., Wang, S., & Tu, Y. (2017). Effects of copper ions on the characteristics of egg white gel induced by strong alkali. *Poultry Science, 96*(11), 4116–4123. https://doi.org/10.3382/ps/pex213

Sheng, L., Wang, Y., Chen, J., Zou, J., Wang, Q., & Ma, M. (2018). Influence of high-intensity ultrasound on foaming and structural properties of egg white. *Food Research International, 108*, 604–610. https://doi.org/10.1016/j.foodres.2018.04.007

Su-IL, P., & Zhao, Y. (2004). Incorporation of a high concentration of mineral or vitamin into chitosan-based films. *Journal of Agricultural and Food Chemistry, 52*, 1933–1939. https://doi.org/10.1021/jf034612p

Tarhan, O., Spotti, M. J., Schaffter, S., Corvalan, C. M., & Campanella, O. H. (2016). Rheological and structural characterization of whey protein gelation induced by enzymatic hydrolysis. *Food Hydrocolloids, 61*, 211–220. https://doi.org/10.1016/j.foodhyd.2016.04.042

Totosaus, A., Montejano, J. G., Salazar, J. A., & Guerrero, I. (2002). A review of physical and chemical protein-gel induction. *International Journal of Food Science and Technology, 37*, 589–601. https://doi.org/10.1046/j.1365-2621.2002.00623.x

Xue, H., Xu, M., Liao, M., Luo, W., Zhang, G., Tu, Y., & Zhao, Y. (2021). Effects of tea and illicium verum braise on physicochemical characteristics, microstructure, and molecular structure of heat-induced egg white protein gel. *Food Hydrocolloids, 110*. https://doi.org/10.1016/j.foodhyd.2020.106181

Xue, H., Xu, M., Zhang, G., Feng, F., Wang, Y., Cao, D., … Zhao, Y. (2021). Effects of stewing with tea polyphenol on the gel properties, microstructure, and secondary structure of boiled egg white. *Journal of Food Science, 86*(10), 4262–4274. https://doi.org/10.1111/1750-3841.15919

Yao, K., Guo, W., Yao, Y., Wu, N., Xu, M., Zhao, Y., & Tu, Y. (2022). Properties, digestion and peptide release of heat-induced duck egg white. *Lwt, 154*. https://doi.org/10.1016/j.lwt.2021.112788

Yoshinori, M., Tatsushi, N., & Noriyuki, H. (1990). Thermally induced changes in egg white proteins. *Journal of Agricultural and Food Chemistry, 38*, 2122–2125. https://doi.org/10.1021/jf00102a004

Yu, L., Xiong, C., Li, J., Luo, W., Xue, H., Li, R., … Zhao, Y. (2020). Ethanol induced the gelation behavior of duck egg whites. *Food Hydrocolloids, 105*. https://doi.org/10.1016/j.foodhyd.2020.105765

Zang, J., Zhang, Y., Pan, X., Peng, D., Tu, Y., Chen, J., … Yin, Z. (2023). Advances in the formation mechanism, influencing factors and applications of egg white gels: A review. *Trends in Food Science & Technology, 138*, 417–432. https://doi.org/10.1016/j.tifs.2023.06.025

Zhang, P., Liu, L., Huang, Q., Li, S., Geng, F., Song, H., … Wu, Y. (2024). Mechanism study on the improvement of egg white emulsifying characteristic by ultrasound synergized citral: Physicochemical properties, molecular flexibility, protein structure. *Ultrasonics Sonochemistry.*. https://doi.org/10.1016/j.ultsonch.2024.107104

Zhao, Y., Cao, D., Shao, Y., Xiong, C., Li, J., & Tu, Y. (2020). Changes in physico-chemical properties, microstructures, molecular forces and gastric digestive properties of preserved egg white during pickling with the regulation of different metal compounds. *Food Hydrocolloids, 98*. https://doi.org/10.1016/j.foodhyd.2019.105281

Zhao, Y., Chen, Z., Li, J., Xu, M., Shao, Y., & Tu, Y. (2016a). Changes of microstructure characteristics and intermolecular interactions of preserved egg white gel during pickling. *Food Chemistry, 203*, 323–330. https://doi.org/10.1016/j.foodchem.2016.02.044

Zhao, Y., Chen, Z., Li, J., Xu, M., Shao, Y., & Tu, Y. (2016b). Formation mechanism of ovalbumin gel induced by alkali. *Food Hydrocolloids, 61*, 390–398. https://doi.org/10.1016/j.foodhyd.2016.04.041

Zhao, Y., Tu, Y., Li, J., Xu, M., Yang, Y., Nie, X., … Du, H. (2014). Effects of alkaline concentration, temperature, and additives on the strength of alkaline-induced egg white gel. *Poultry Science, 93*(10), 2628–2635. https://doi.org/10.3382/ps.2013-03596

Zhou, H., Hu, X., Xiang, X., & McClements, D. J. (2023). Modification of textural attributes of potato protein gels using salts, polysaccharides, and transglutaminase: Development of plant-based foods. *Food Hydrocolloids, 144*. https://doi.org/10.1016/j.foodhyd.2023.108909